Energy 42 (2012) 251–260

Contents lists available at SciVerse ScienceDirect

Energy

journal homepage: www.elsevier.com/locate/energy

Solar thermochemical production of ammonia from water, air and sunlight: Thermodynamic and economic analyses

Ronald Michalsky [a,b], Bryon J. Parman [a,c], Vincent Amanor-Boadu [c], Peter H. Pfromm [b,*]

[a] NSF IGERT, Kansas State University, Manhattan, KS 66506, USA
[b] Department of Chemical Engineering, Kansas State University, Manhattan, KS 66506, USA
[c] Department of Agricultural Economics, Kansas State University, Manhattan, KS 66506, USA

ARTICLE INFO

Article history:
Received 31 October 2011
Received in revised form
20 February 2012
Accepted 27 March 2012
Available online 30 April 2012

Keywords:
Hydrogen
Methane
Fertilizer
Electricity
Economics
Infrastructure

ABSTRACT

Ammonia is an important input into agriculture and is used widely as base chemical for the chemical industry. It has recently been proposed as a sustainable transportation fuel and convenient one-way hydrogen carrier. Employing typical meteorological data for Palmdale, CA, solar energy is considered here as an inexpensive and renewable energy alternative in the synthesis of NH_3 at ambient pressure and without natural gas. Thermodynamic process analysis shows that a molybdenum-based solar thermochemical NH_3 production cycle, conducted at or below 1500 K, combined with solar thermochemical H_2 production from water may operate at a net-efficiency ranging from 23 to 30% (lower heating value of NH_3 relative to the total energy input). Net present value optimization indicates ecologically and economically sustainable NH_3 synthesis at above about 160 tons NH_3 per day, dependent primarily on heliostat costs (varied between 90 and 164 dollars/m^2), NH_3 yields (ranging from 13.9 mol% to stoichiometric conversion of fixed and reduced nitrogen to NH_3), and the NH_3 sales price. Economically feasible production at an optimum plant capacity near 900 tons NH_3 per day is shown at relative conservative technical assumptions and at a reasonable NH_3 sales price of about 534 ± 28 dollars per ton NH_3.

© 2012 Elsevier Ltd. All rights reserved.

1. Introduction

The U.S. Census Bureau estimates that between 1900 and 2000, the world's population grew from 1.6 billion to 6.0 billion, and is projected to reach 9.0 billion by 2050 [1]. Global human population growth is projected to increase the strain on current natural resources, such as land, fossil hydrocarbons, and fresh water, if technological advances are not made in the production of products and services using these resources.

While technological advances in agriculture in the 20th century - chemical fertilizers, mechanization, breeding, genetic improvement, chemical pest control, processing and storage systems - have contributed to vastly increase the productivity of land globally, the interface between energy and fertilizer production, especially ammonia, promises to challenge the agricultural productivity in the future. At present, over 100 million metric tons of NH_3 [2] are produced annually, driven by increasing food demand and the need for higher crop yields [3]. NH_3 is the single-most important synthetic fertilizer, accounting for 58 wt% of all fertilizer consumed for example in the USA in 2007 [4]. Its role in the production of bio-energy feedstock and its potential use in solar-derived H_2 storage [5–7] or as a liquid fuel [8,9] augment its criticality and importance in the global economy.

NH_3 easily reaches the U.S. Department of Energy 2015 hydrogen storage target for H_2-based transportation fuels [8,10] or it can be blended into diesel for direct combustion in modified diesel engines releasing mainly H_2O and N_2 as combustion-products [11]. If these competitive uses and the duty of the agricultural industry to feed a growing global population at reasonable prices are to be realized new and innovative NH_3 synthesis technology will likely be required.

Industrially, the Haber–Bosch process synthesizes NH_3 by shifting the reaction equilibrium of a N_2/H_2 gas mixture at high pressure (about 30 MPa) towards formation of ideally 22.7 mol% NH_3 (relative to stoichiometric conversion) at 673–873 K and in presence of a catalyst [12]. The energy-intensive process [13], including natural gas/steam reforming for H_2 production (accounting for approximately 84% of the total energy required), consumes 28–40 GJ/t NH_3 in form of natural gas [12,14] (about

* Corresponding author. 1036 Durland Hall, Kansas State University, Manhattan, KS 66506. Tel.: +1 785 532 4312; fax: +1 785 532 7372.
E-mail address: pfromm@ksu.edu (P.H. Pfromm).

0360-5442/$ – see front matter © 2012 Elsevier Ltd. All rights reserved.
doi:10.1016/j.energy.2012.03.062

1–2% of the world's annual energy production [15]). Approximately 2.3 t of fossil-derived CO_2 are generated per t NH_3 synthesized [14]. Employing steam-reforming of coal increases the energy required for NH_3 production even further (about 47.6–165.9 GJ/t NH_3) and increases the associated generation of fossil CO_2 (16.7 t CO_2/t NH_3) [6,14]. Economies of scale have dictated current Haber–Bosch facilities producing above about 1500 t NH_3 per day, consuming significant quantities of natural gas and influencing that commodity's price trend. This in turn has a direct impact on NH_3 prices and their volatility.

Various alternatives proposed for nitrogen fixation from the atmosphere via synthesis of NH_3 including catalytic formation of NH_3 near ambient temperature and pressure in the liquid phase [16] and electrochemical NH_3 synthesis [17] have not yet reached maturity. Solar thermochemical NH_3 synthesis at ambient pressure is a proposed remedy to some of the difficulties associated with the Haber–Bosch process [5,18–21]. Reactive NH_3 synthesis via a two-step solar thermochemical cycle of metal oxide nitridation and metal nitride hydrolysis [19,22] has been demonstrated to form significant quantities of NH_3 from air and water at near 0.1 MPa [19]. The process neither requires a catalyst nor a fossil hydrogen source. The energy required for the generation of H_2 via H_2O splitting and for the reductive cleavage of N_2 is supplied in form of solar energy [18,20]. Concentrated solar radiation, absorbed at elevated temperature in an endothermic metal oxide reduction, creates a metal nitride in the presence of N_2. The fixed nitrogen is, thereafter, released from the solid metal nitride as NH_3 in an exothermic steam hydrolysis reaction. Given the abundance of solar radiation in many areas of the world, this approach has the potential to produce NH_3 sustainably and facilitates simultaneously storage of intermittently available solar energy [23,24].

Solid carbon (biomass or charcoal) has been suggested as reducing agent of the metal oxide in the process discussed above [18,20]. However, carbon may not be available in the right quantities and proximity to the manufacturing plant, requiring transportation or production, using up arable land, and requiring expensive and energy-intensive processing [25,26]. On the other hand, reactants forming metal oxides which can be reduced with H_2 unfortunately tend to not fix 0.1 MPa N_2 in form of metal nitrides and show low NH_3 yields when reacting their nitrides with steam [21]. Molybdenum considered here represents a trade-off [21]: The oxide (MoO_2) that is formed during nitride (Mo_2N) hydrolysis at above 800 K can be reduced [27] and nitridated with moderate yields in H_2/N_2 gas mixtures in the range of 800–1500 K [28,29]. Given the relative high ionicity of the nitride [30,31], significant quantities of NH_3 are liberated during the hydrolysis of Mo_2N at atmospheric pressure.

The work presented here conceptually assesses the technical and economic attractiveness of Mo-based solar thermochemical NH_3 synthesis in the absence of any carbonaceous material or natural gas as feedstock or for energy (Fig. 1). Experimentation towards the technical feasibility of the reaction cycle is described elsewhere [20].

A thermodynamic analysis for synthesizing NH_3 in a two-step solar thermochemical reaction cycle from H_2 and N_2 with a Mo-based reactant at 0.1 MPa (Fig. 1) is presented in Section 2.1. Section 2.2 determines plant capacity and energy efficiency and CO_2 emissions of the Haber–Bosch process implemented with natural gas as a benchmark for a process analysis of the proposed reaction cycle (Fig. 2) in Section 2.3. The analysis simulates an implementation of the reaction cycle with H_2 generated via a well-studied solar thermochemical H_2O splitting cycle using zinc [24,32,33]. In practice, the proposed NH_3 synthesis may be implemented with other solar-to-hydrogen technologies [33]. Section 3.1

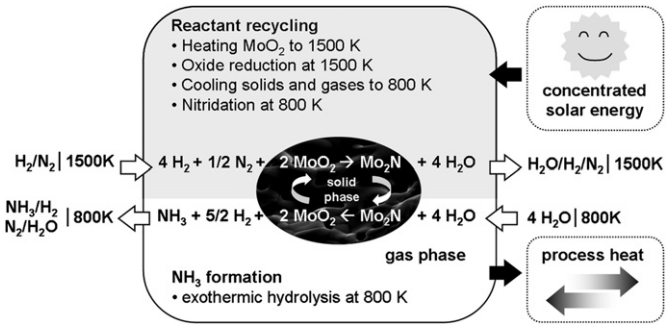

Fig. 1. Concept for solar thermochemical NH_3 synthesis near atmospheric pressure using a molybdenum reactant.

estimates investment costs for unit operations and chemical commodities used in Section 3.2 that develops an economical optimization model for scalable solar thermochemical NH_3 synthesis. The model is evaluated and discussed employing net present value calculations in Section 3.3. Section 3.4 shows that the proposed concept is economically attractive under fairly conservative assumptions.

2. Thermochemical NH_3 synthesis cycle

The Gibbs free energy of formation for a metal nitride is relatively small compared to the corresponding oxide. Thus, only a few metals such as Mo allow simultaneously for oxide reduction with H_2 and reductive cleavage of dinitrogen at 0.1 MPa [21,28,29]. Mo is shown here to be a promising reactant for solar thermochemical NH_3 synthesis.

To estimate the equilibrium reaction yield achievable in a system closed to mass transfer, the free energy of reaction, $\Delta_{rxn}g$, was computed based on the literature [27]. The absolute error of energy of formation data was estimated previously with ±3 kJ [34] and was taken as 2% of the value in kJ/mol. The computed formation of Mo_2N was extrapolated at >800 K using a linear fit ($R^2 > 0.999$). With the free energy computations in hand, the equilibrium constants, K_{eq}, were determined at atmospheric pressure taking the total number of chemical species in the system for simplicity as the arithmetic mean of the number of reactants and the number of products at complete conversion [35]. This allows solving the elemental mol balances of the given reaction system symbolically ("live" Symbolics, Mathcad 13) as a function of K_{eq}, that is yielding the equilibrium composition of the reaction system as a function of temperature, T, at 0.1 MPa.

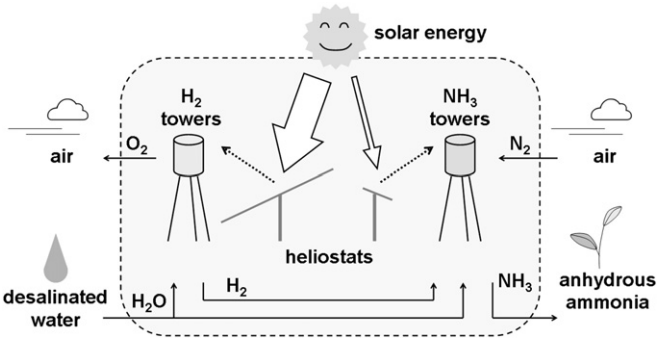

Fig. 2. Conceptual implementation of solar thermochemical NH_3 synthesis coupled with solar thermochemical H_2 synthesis.

2.1. Thermodynamic analysis

Conversion of solar energy is accomplished by thermochemical reduction of Mo(IV) oxide with H_2 to Mo metal (Eq. (1)):

$$2MoO_{2\,(s)} + 4H_2 \leftrightarrow 2Mo_{(s)} + 4H_2O \quad \Delta_{rxn}h_{1500K} \approx 130 \pm 25\ kJ/mol\ N \tag{1}$$

$\Delta_{rxn}g$ of Eq. (1) indicates that the reaction equilibrium is favored thermodynamically at above ca. 1428 K (Fig. 3A). The chemical energy stored in the endothermic metal formation (the enthalpy of reaction, $\Delta_{rxn}h$ [27]) allows subsequently for slightly exothermic N_2 fixation in form of metal nitridation (Eq. (2)) favorably at lower temperatures (Fig. 3B):

$$2Mo_{(s)} + 1/2N_2 \leftrightarrow Mo_2N_{(s)} \quad \Delta_{rxn}h_{800K} \approx -63.2 \pm 0.8\ kJ/mol\ \ N \tag{2}$$

The yield (Y = mol solid reaction product formed/mol solid product at stoichiometric conversion) for reaction 1 or 2 is below stoichiometric conversion at thermodynamic equilibrium (Eq. (1) at ca. 1428 K, Eq. (2) at ca. 1115 K, assuming 0.1 MPa) (Fig. 3). However, given the non-equilibrium situation (mass exchange) in an actual flow-through reactor, and assuming a high effective reactant surface, stoichiometric conversion for both reactions is assumed below. The over-stoichiometric supply of H_2 (Section 2.3), may account for excess MoO_2 formed during nitride hydrolysis from Mo that may not have converted to Mo_2N during the nitridation.

The fraction of reactive nitrogen ions yielded in the solid state due to the electron transfer between bonding Mo 4d, Mo 5s and N 2p orbitals allows for exothermic formation of NH_3 when the nitrogen in the solid phase is substituted with more electronegative oxygen (Eq. (3)):

$$Mo_2N_{(s)} + 4H_2O \leftrightarrow 2MoO_{2\,(s)} + NH_3 + 5/2H_2 \quad \Delta_{rxn}h_{800K} \approx -168 \pm 29\ kJ/mol\ N \tag{3}$$

Uncharged N^0 in the interstitial space of the metal or metal nitride crystal may form N_2 upon nitride corrosion (Eq. (4)):

$$Mo_2N_{(s)} + 4H_2O \leftrightarrow 2MoO_{2(s)} + 1/2N_2 + 4H_2 \quad \Delta_{rxn}h_{800K} \approx -114 \pm 29\ \ kJ/mol\ \ N \tag{4}$$

The assumptions below (see 2.3) are based on experimental results (manuscript in preparation) for hydrolysis of 25.5 ± 0.5 wt% Mo_2N powder (balance Mo, 17 ± 8 μm average particle diameter, 429 ± 3 m^2/kg BET surface area) at 773 K with steam supplied for 1 h at a rate of 0.91 ± 0.02 $ml_{(STP)}$/min. The simulation assumes either Y_3 = 100 mol%, Y_4 = 0 (stoichiometric conversion), or Y_3 = 13.9 mol%, Y_4 = 9.1 mol%. Decreasing the hydrolysis temperature (Fig. 4) or increasing the availability of effective reactive surface sites may allow increasing the yield of NH_3 in practice. Endothermic decomposition of Mo_2N (Eq. (2), when favoring the species on the left side) was neglected at this point due to a positive $\Delta_{rxn}g$ at 800 K. Oxidation of MoO_2 to MoO_3 [28] is not favored at equilibrium (105.2 kJ/mol oxide $\Delta_{rxn}g$ at 800 K [27]) but driven when the equilibrium is not established due to MoO_3 vapor formation (MoO_3 boils at about 1428 K). This can be reduced or avoided by low hydrolysis temperatures, low steam flow rates and short reaction times.

The overall reaction represents an alternative for realizing the Haber–Bosch reaction ($1/2N_2 + 3/2H_2 \leftrightarrow NH_3$) near 0.1 MPa. The enthalpy required for breaking the N_2 triple bond is supplied indirectly in form of concentrated solar radiation providing the heat (at 1500 K) for the endothermic reduction of Mo(IV) oxide to Mo metal (Eq. (1)). The metal is utilized to cleave and thermochemically reduce dinitrogen (Eq. (2)) increasing the metallic oxidation state formally to $Mo^{+3/2}$ in Mo_2N [30,31]. Mo_2N is further oxidized to Mo(IV) when reacted with H_2O to liberate NH_3 (Eq. (3)). The heat released from Eqs. (2)–(4) is partly integrated [36] (see 2.3). The significant amount of energy required to form H_2 from H_2O (Fig. 2) is supplied as solar radiation at 2000 K employing a two-step solar thermochemical cycle of endothermic ZnO dissociation (about 679.2 kJ per 3/2 mol H_2 $\Delta_{rxn}h$ at 2000 K), quenching of the Zn/O_2 vapor leaving the reactor, and exothermic oxidation of the condensed Zn with H_2O at 400 K (about −156.6 kJ per 3/2 mol H_2 $\Delta_{rxn}h$ at 400 K) recycling ZnO and producing H_2 (both computed at 0.1 MPa and assumed with stoichiometric conversion). This well-studied cycle has been discussed elsewhere [24,32].

2.2. The scale of industrial NH_3 synthesis

As a benchmark, the Aspen Plus (V7.0) Ammonia Model [37] was used to simulate the industrial NH_3 production using natural gas as a feedstock. The model comprises a reforming unit converting a desulfurized hydrocarbon feed with steam (primary reformer, 3.1–3.3 MPa, 775–1064 K) and air (secondary reformer, 2.9–3.1 MPa, 1251–1530 K) into H_2 and carbon oxides. Subsequently, CO is converted catalytically (2.7–2.9 MPa, 483–721 K) to CO_2 that is removed with NH_3 forming an ammonium hydrogen carbonate byproduct. The synthesis gas obtained is freed from traces of CO and CO_2 employing a nickel catalyst to form CH_4 (methanizer). Thereafter, NH_3 is synthesized at 28.4–29.2 MPa and 686–799 K over a promoted iron catalyst. The major fraction of the 23.9 mol%

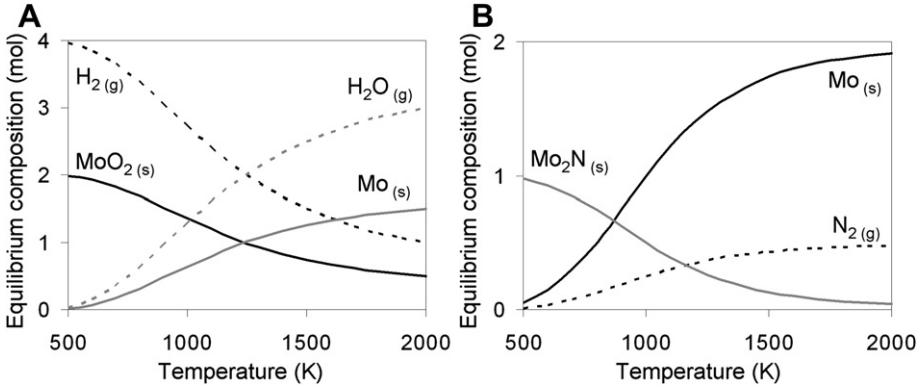

Fig. 3. To assess the temperatures that are required for thermodynamic feasibility of the reaction cycle proposed: equilibrium composition of (A) MoO_2 reduction (Eq. (1)) and (B) N_2 fixation via Mo nitridation (Eq. (2)) (see 2.1) as a function of temperature at 0.1 MPa.

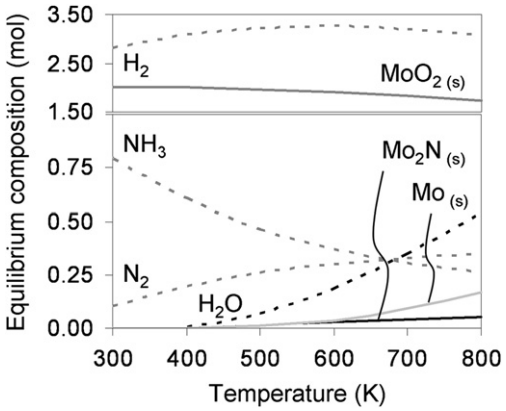

Fig. 4. To assess the temperatures that are required for thermodynamic feasibility of the reaction cycle proposed: equilibrium composition of Mo_2N hydrolysis forming MoO_2, NH_3 and H_2 (Eq. (3)), Mo_2N oxidation forming MoO_2, N_2, and H_2 (Eq. (4)) and thermal dissociation of Mo_2N forming Mo and N_2 (see 2.1) as a function of temperature at 0.1 MPa.

NH_3 in the synthesis loop (about 33.9 mol% nitrogen–to–NH_3 conversion) is liquefied via refrigeration (27.5 MPa, 288–304 K) and stored at 3 MPa. The model estimates the thermodynamic properties of gases at high temperature and pressure using a modified Redlich–Kwong equation of state (RKS-BM). Liquid and vapor properties in the CO_2 scrubbing unit are modeled with an electrolyte NRTL or a Redlich–Kwong equation of state model respectively. A detailed description of the Haber–Bosch modeling is provided elsewhere [37].

Overall, the process converts approximately 35.9 t/h natural gas (80.0 mol% CH_4, 17.7 mol% C_2H_6, balance hydrocarbons and air, at 3.8 MPa and 303 K) with 308.5 t/h air at 302 K and 69.0 t/h water at 293 K (both at 0.1 MPa) to 27.5 t/h liquid anhydrous ammonia (99.6 mol% NH_3, 2 MPa, 306 K), 126.9 t/h ammonium bicarbonate salt (98.7 mol% NH_4HCO_3, 0.1 MPa, 293 K), and 259.0 t/h flue gas (7.0 mol% CO_2, 16.1 mol% H_2O, balance N_2, O_2, and Ar, 0.1 MPa, 333 K). To compare this to the discontinuous operation of the solar thermochemical NH_3 synthesis in Section 2.3, this equates production of about 1324 t NH_3 per day (as anhydrous ammonia or ammonium salt, assuming 24 h/d operation).

The enthalpy balance of the process indicates a net heat duty of about 289 MW, mainly due to the heat required in the reforming unit and the CO_2 stripper and the electricity consumed for synthesis gas compression. Taking the lower heating value (LHV) of natural gas at 31.89 GJ/t [38] results in further consumption of about 32.6 t/h natural gas and 549.7 t/h air generating 582.3 t/h flue gas (9.9 mol % CO_2, 18.3 mol% H_2O, balance N_2 and Ar). This yields total CO_2 emissions of the process - flue gas - at about 2.17 t CO_2 per t NH_3. The energy efficiency can be estimated with 46.9% (the LHV of 1324 t/d NH_3 relative to the LHV of 1644 t/d natural gas).

2.3. Numerical process analysis

Given its conceptual state a conceivable solar thermochemical process that is converting air, desalinated water, and sunlight into liquid ammonia and compressed oxygen (Fig. 5) was analyzed similar to other thermochemical processes reported in the literature [23,36,39]. To estimate the plant layout mass and energy balances were solved iteratively (Generalized Reduced Gradient nonlinear optimization code, 10^2 iteration steps, 10^{-4} minimum sensitivity, Excel 2003) at steady-state and as a function of a variable NH_3 capacity. Two scenarios were computed: First, assuming $Y_3 = 100$ mol%, $Y_4 = 0$ (see 2.1), and the ratio of gaseous reactant required at minimum to the amount of gaseous reactant supplied to any reaction, r_{gas}, of 90 mol%, "ideal operation". The second, rather "conservative operation", assumes $Y_3 = 13.9$ mol%, $Y_4 = 9.1$ mol%, and $r_{gas} = 67$ mol%.

To analyze the performance of the envisioned plant located in a suitable geographic region typical meteorological data from the updated National Solar Radiation Data Base (NSRDB) [40,41] was used. The hourly direct normal irradiance values provided by the database were averaged over a typical meteorological year to identify several regions in the southwestern U.S. with an averaged

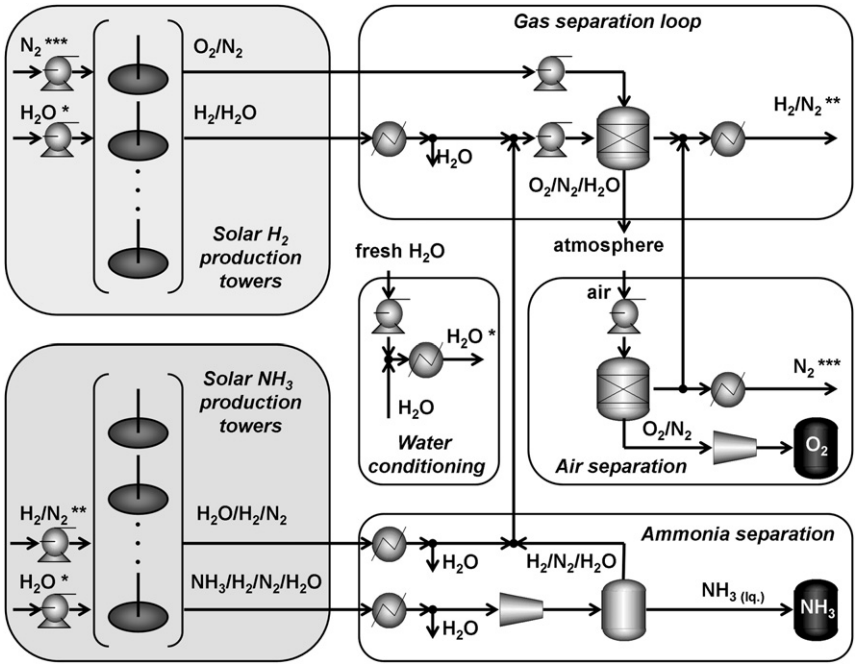

Fig. 5. Process schematic of solar thermochemical NH_3 synthesis and on-site H_2 production (dry cooling system not shown).

normal irradiance in the range of 7.01–7.81 kWh/m^2/d. The analysis presented here assumes a yearly-averaged direct normal irradiance of 7.48 kWh/m^2/d (that is 1 kW/m^2 for annualized 7.48 h/d), based on data for 1997–2005, Palmdale Airport, CA, USA (approximately 80 km linear distance to the Pacific).

Solar radiation is concentrated via heliostats and absorbed at 1500 or 2000 K respectively (Fig. 5) with an efficiency of solar radiation converted to chemical reaction heat (dimensionless mean flux concentration ratio at 10^4, for a detailed description see [24]) assumed at 0.78 (Fig. 6). The radiation is received by a series of reactors at 100 m above ground (similar in appearance to the Solar Two power tower, Mojave Desert, CA, USA, or the PS10 and PS20 plants near Seville, Spain) splitting H_2O into H_2 and O_2 ($2.5 \times 2.5 \times 5.0$ m reactor volume, V_R, Mo-alloy), or converting H_2 and N_2 to NH_3 ($15 \times 15 \times 25$ m V_R, ceramic lining). V_R was estimated assuming 1 min residence time of the gaseous species at a given temperature in the reactor (using a molar ratio of N_2 sweep gas to ZnO of 0.1 [32]). In practice V_R will be determined empirically by reaction kinetics for a reactant with optimized composition and by the heliostat area required per reactor for providing heat at a desired temperature.

Sensible, $\Delta_{sen}h$, and latent, $\Delta_{lat}h$, heat and the $\Delta_{rxn}h$ of exothermic reactions [27] are recovered and integrated at a ratio of 0.6 (that is heat losses at about 40%) [36] estimating heat exchange areas of 1.44×10^4 m^2 for temperatures up to 2000 K (lined with molybdenum disilicide) or 8.47×10^4 m^2 < 1500 K (Fig. 6). This is assuming replication of the production described in Section 2.2. The remaining heat is removed via dry (air) cooling (5.71×10^5 m^2 heat exchange area, 40 K effective ΔT_{air}, 2 kPa pressure losses [42], efficiency of fans and compressors assumed with 0.86 [43]). Although shown to be by a factor of 4–6 more energy-intensive and by a factor of 4–12 more capital-intensive than wet cooling, dry cooling was employed due to the crucial role of water availability [44].

The N_2 is required only at industrial-grade purity (as sweep gas and feedstock) and is produced via membrane permeation (based on literature values for gas permeability and diffusivity for polysulfone fibers [45]) yielding at 0.2 MPa trans-membrane pressure an effective membrane area of ca. 8.48×10^5 m^2. By-product O_2 (Table 1) is compressed isentropically and stored. NH_3 is separated from its synthesis vapor and liquefied via cooling and compression to 306 K and 2 MPa (see 2.2) and stored in steel tanks. H_2 and N_2 gas mixtures recovered from the NH_3 synthesis cycle are enriched with H_2 generated in the H_2 synthesis cycle and desiccated with a silica gel bed (0.4 g H_2O/g SiO_2 adsorption capacity [46], 200 K maximum ΔT_{gas} between H_2O ad- and desorption, 10 kPa pressure drop assumed for all solid beds). Traces of Ar, CO_2, and Zn or MoO_3 vapor have been neglected for simplicity.

Given the net energy content of NH_3 and neglecting the energy stored in the separation of O_2 from air, conversion of solar energy to NH_3 was estimated with an efficiency of about 23–30% at maximum (LHV of NH_3 relative to the total energy requirement, including net electricity as solar heat-equivalent, for conservative or ideal operation respectively) (Table 1). This energy is released in form of heat when NH_3 is combusted (e.g., as transportation fuel) [11] or in form of H_2 when NH_3 is used as a single-use hydrogen carrier [6,7,9]. The maximum efficiency as estimated is below 46.9% estimated for the NH_3 synthesis with natural gas at this scale (Section 2.2) but within the range estimated for the industrial NH_3 synthesis via steam reforming with natural gas or coal respectively, i.e., 11–66% (Table 1).

The total electricity required for the proposed process (assuming as a worst-case scenario all grid-electricity is generated from coal-fired power plants emitting 0.91 t CO_2/MWh [47]) results in CO_2 emissions in the range of 0.62–1.08 t CO_2/t NH_3. That is a net reduction of fossil CO_2 emissions by 50–71% relative to the current NH_3 synthesis with natural gas (see 2.2) or up to 96% relative to the industrial NH_3 synthesis with coal (see 1.).

Table 1
Mass balance and total heat and electricity input.

Overall process mass balance			
	m (t/d)	T (K)	p (MPa)
Raw materials			
Air	1970	300	0.1
Water	2418	293	0.1
Products			
NH_3 (99 wt% NH_3 in H_2O)	1344	306	2
O_2 (82 wt% O_2 in N_2)	555	300	15
air (75 wt% O_2, 12 wt% H_2O)	2489	413	0.1

Comparison of total energy requirements (GJ/t NH_3)	
Solar thermochemical NH_3[a]	56.4–70.6
Natural gas/steam reforming & Haber–Bosch[b]	28–40.1
Coal gasification & Haber–Bosch[c]	47.6–165.9
Lower heating value (LHV) of NH_3[d]	18.6
Gibbs free energy of mixing for O_2 separation	0.2

[a] Ideal operation (Y_3 = 100 mol%, Y_4 = 0 mol%, r_{gas} = 90 mol%, see 2.1) to conservative operation (Y_3 = 13.9 mol%, Y_4 = 9.1 mol%, r_{gas} = 66.7 mol%, see 2.1);
[b] Taken from [14] and see 2.2;
[c] Ref. [6,14];
[d] Ref. [49].

3. Economic feasibility

The production of NH_3 presented in Section 2 comprises two phases: (i) H_2 generation via a two-step solar thermochemical H_2O splitting cycle, and (ii) solar thermochemical NH_3 synthesis from desalinated water, air and H_2. It is envisioned that the required solar energy is harvested with an array of heliostats concentrating solar radiation that is received by a reactor placed atop a central collector tower, i.e., "H_2 towers" if generating H_2, or "NH_3 towers" if generating NH_3 (Figs. 2 and 5).

If the production described in Section 2.2 is to be replicated by this process at "ideal operation", it will require 33.2 t Mo, 17.0 t Zn, 0.48 km^2 lens area for concentration of sunlight, A_{lens}, utilized by the NH_3 synthesis cycle, and 2.95 km^2 A_{lens} utilized by the H_2 synthesis cycle (Fig. 5). On the other hand, "conservative operation" would lead to 239.1 t Mo, 17.0 t Zn, 1.11 km^2 A_{lens} to synthesize NH_3, and 3.10 km^2 A_{lens} to produce H_2. The increased amount of Mo does not significantly affect capital costs (see 3.1). However, the increased land requirements (increased totally by 22.7% for provision of sensible and latent heat and $\Delta_{rxn}h$ of Eq. (1)) under the "conservative operation" lead to a significantly increased amount of capital that needs to be raised for reactors and solar concentrators. A process summary is given in Table 1 and Fig. 6.

3.1. Data sources

The mass and energy balances were utilized to generate a generic list of components and equipment required for realizing the proposed process (see 2.3). Data estimates as realistic as possible were obtained from equipment manufacturers, service providers and operating facilities. A summary for fixed costs dependent on or independent of the NH_3 capacity or operational costs is given in Table 2, 3 or 4 respectively.

The operating costs including heliostat maintenance and service are assumed at 3% of total heliostat costs. Labor is assumed based upon plant size and skill level. Air compressors and water pump costs are based upon gas/liquid mass flow and stream conditions. Variable costs are assumed to grow at an annual inflation rate of 3%. Corporate income tax is set and maintained at its current level of

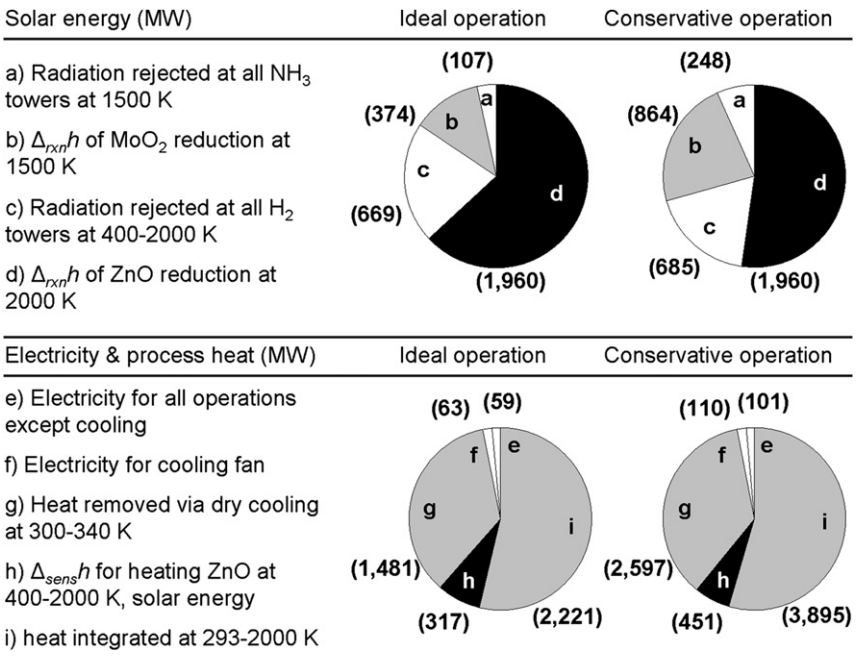

Fig. 6. Total power requirements at industrial production scale (producing 1324 t NH_3 per day, within 7.48 h/d operation on average, see 2.1, 2.2 and 2.3). All power values given in brackets are in MW/plant.

35%. NH_3 price is forecast using 10^3 Monte Carlo simulations based on a 20-year historical mean and standard deviation of U.S. prices (Fig. 7). The projected NH_3 price series drawn from the Monte Carlo model has a mean, median, or standard deviation of 522, 531 or 27 dollars/t NH_3 respectively. It is assumed that variable costs per unit will be linear in production, with scale effects influencing the linearity of per unit cost over different production levels.

3.2. Economics of solar thermochemical NH_3 production

The economics do not assume any kind of regulatory or public support for the technology proposed here. No credit is taken or subsidies are assumed for reduction of CO_2 emissions, use of renewable vs. non-renewable resources in making the product, etc.

The NH_3 plant is assumed to be a profit-maximizing/cost minimization business. Thus, it will select its fixed and variable costs to produce at an output level that maximizes the return to its investment. This assumption implies that a principal constraint in building such a plant is available capital, treating costs of capital as part of operating costs. Economic theory suggests that the plant would be built if it is economically feasible. Economic feasibility is defined here to mean the ability of the plant to return a positive net present value at a specified discount rate over a reasonable lifespan of the project. "Reasonable lifespan" is defined to imply a period prior to the need for major capital retrofitting of the plant, assumed in this case to be 20 years.

An optimization approach is adopted to evaluate the economic feasibility of building a solar thermochemical NH_3 production plant

Table 2
Cost estimates and necessary quantities for each NH_3 and H_2 tower (scenario 1 conditions, M marks million, websites information retrieved in April 2011, HX abbreviates heat exchanger). Total costs can be found by the product of each quantity column element and its related cost per unit.

Item category	Unit	Cost per unit (U.S. dollars)	Quantity per NH_3 tower	Quantity per H_2 tower	Primary source
Mo reactant	kg	36,000	1174		http://www.lme.com/minormetals/
Zn reactant	kg	234		2288	http://www.lme.com/zinc.asp
Silica gel	kg	211	59		http://www.ecvv.com/product/2427724.html
NH_3 reactor	each	8.0 M	1		Mark Jensen, CF Industries, Plant Manager (April 8, 2011)
H_2 reactor	each	16.0 M		1	
Water tank	each	0.6 M	0.16		Wayne French, VP Tank Builders Inc. (April 8, 2011)
Piping	m	69	199		http://www.saginawpipe.com/steel_pipe_chart-3.htm
Water pumps	each	30,000		1.4	Assumed
Helistats	m^2	164	17,006	397,039	Kolb, G. et al., 2006 Heliostat Cost Reduction", project working paper
Land	m^2	4.9 M	21,257	496,299	Southern California location assumed, http://www.bajarealestategroup.net/baja_real_estate/viewcategory/6/
Support tower	each	1.3 M	1	1	Mid-Atlantic Regional Space Port. Wallops Island, VA, Construction Manager (April 5, 2011)
HX < 2000 K	m^2	467		1944	Dennis L. Youchison, Sandia National Lab., Fusion Technology, Albuquerque, NM
HX < 1500 K	m^2	467	2992		
HX < 500 K	m^2	50	20,160		
Air separation	each	0.8 M	0.14		John Font, Innovative Gas Systems (April 6, 2011)
Trucks or trailers	each	0.3 M	0.59		Assumed
Blowers	each	30,000	0.78		
Storage tanks	m^2	60		139.4	http://metalbuildingdepot.com/specials/default.aspx
Engineering costs		10%			Assumed at 10% total tower construction cost

Table 3
Costs of each fixed plant component independent of scale.

Item category	Cost per item (million U.S. dollars)	Primary source
Compressor (NH_3)	0.15	Mark Jensen, CF Industnes, Plant Manager (April 8, 2011)
Compressor (O_2)	0.15	Assumed
Compressor (air)	0.10	Assumed
Blower (silica bed)	0.03	Assumed
Storage container (NH_3)	10.00	Mark Jensen, CF Industnes, Plant Manager (April 8, 2011)
Storage container (O_2)	14.00	Mark Jensen, CF Industnes, Plant Manager (April 8, 2011)
Master control system	3.0	http://www.solarpaces.org/CSP_Technology/docs/solar_tower.pdf (April, 2011)

using the foregoing technology. This approach is particularly helpful because of the physical plant constraints in the production process and the direct effects of these constraints on the plant's profitability. It is assumed that the output of NH_3 in each scenario, Z_{lm}, is defined as:

$$Z_{lm} = \delta_{lm} X_N, \quad l = 1,2;\ m = 1,2 \tag{5}$$

where δ_{lm} is a yield constant in t/h per tower based on the technical efficiency of the towers, and X_N is the quantity of NH_3 towers (see 3). The objective function of the optimization model is to maximize operational profits, π, by selecting the optimum number of X_N given the expected market price, p, of NH_3 and in cognizance of plant operational costs. The model is evaluated under two operational, l, and cost, m, conditions, yielding four scenarios:

- 1: ideal operation, conservative costs (l, $m = 1$)
- 2: ideal operation, optimistic costs ($l = 1$, $m = 2$)
- 3: conservative operation, conservative costs ($l = 2$, $m = 1$)
- 4: conservative operation, optimistic costs (l, $m = 2$)

Since the only choice variable is X_N, the optimization model may be presented as:

$$\begin{aligned} \max_{X_N} \pi_{lm} &= pZ_{lm}(X_N) - C(Z_{lm}) - F_{Z_{lm}} \\ s.t.\ \ & \rho_l X_N \le X_H \\ K_{lm,j_{lm}} - F_{Z_{lm}} &\ge b_{N_{lm}} X_N + b_{H_{lm}} X_H \\ & X_N, X_H \in [0, \infty) \\ & X_N, X_H \equiv I \end{aligned} \tag{6}$$

where $C(Z_{lm})$ is the variable costs for producing Z output and F_Z is the fixed costs under each scenario. The number of H_2 towers is a fixed proportion, ρ, of the number of NH_3 towers. This constraint is set as an inequality because it is technically feasible to produce more H_2 than required. The second constraint in Eq. (6) stipulates that available capital, K_{lm}, less the associated fixed costs, F_Z, must be higher than the acquisition costs of the two types of central tower systems. Available capital is evaluated j times with particular characteristics to assess the effect of capital on the optimum output and profits. Since the optimization model is essentially choosing output using the number of NH_3 and H_2 towers, it is plausible to present all plant fixed costs, i.e., the coefficients b_{Nlm} and b_{Hlm}, in terms of towers. The final two constraints indicate that the number of towers is always a positive non-zero integer to ensure that production does occur. Table 5 provides a summary of the assumptions underlying the computed scenarios.

With regard to assumed costs, cost and quantity estimates for Scenario 1 - the baseline scenario - are provided in Table 2. Note that the product and sum of each tower specific column and the cost column gives the value of b_{N11} and b_{H11}. In Scenario 2 the heliostat price is decreased from 164 to 90 dollars/m^2 [33] and the price of heat exchangers for temperatures up to 2000 K is reduced by two thirds from 467 to 155 dollars/m^2. This results in an overall cost per tower of 13.9 million dollars per NH_3 tower or 53.3 million dollars per H_2 tower. That is cost reductions relative to Scenario 1 of 3.76 or 28.1 million dollars per NH_3 or H_2 tower respectively. It should be noted that the cost of the NH_3 tower accounts for major components of the overall process (Tables 2 and 4). This shows that the impact of the heliostat investment costs for the H_2 production cycle is quite significant. Correlating linearly with the area estimate for harvesting solar radiation (see 2.3 and Fig. 6), about 74–86%

Table 4
Operating costs per tower. The Master control system labor was assumed at 200,000 dollars. Water cost per ton from [50], electricity cost per MWh from [51], other costs assumed.

Input	Cost (U.S. dollars/ unit)	Quantity per NH_3 tower	Quantity per H_2 tower
Electricity	41.79 MWh^{-1}	1	–
Water	0.8 t^{-1}	–	2.29 t
Labor (reactors)	75,000 $year^{-1}$	1	–
Labor (compressors)	100,000 $year^{-1}$	0.1	–
Labor (piping)	60,000 $year^{-1}$	0.25	–
Service (heliostats)	3% of total heliostat cost	Varies	Varies
Total variable costs (NH_3 tower)	133,747 $year^{-1}$		
Total variable costs (H_2 tower)	1,653,155 $year^{-1}$		

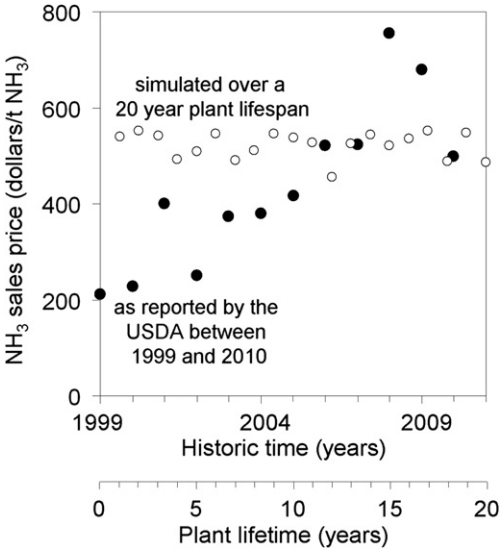

Fig. 7. Actual average annual NH_3 sales price reported by the USDA between 1999 and 2010 (filled circles) and the Monte Carlo 20-year price simulation with a mean of 522.24 dollars/t NH_3 and a standard deviation of 27.13 dollars/t NH_3 (empty circles).

Table 5
Combination of scenario conditions and parameters (M marks million).

Scenario matrix	$l = 1$	$l = 2$
$m = 1$	$\delta = 6.35$ $\rho = 0.262$ $j =$ \$150 M + \$50 M to max(\$1100 M)	$\delta = 2.97$ $\rho = 0.146$ $j =$ \$100 M + \$100 M to max(\$1600 M)
$m = 2$	$\delta = 6.35$ $\rho = 0.262$ $j =$ \$150 M + \$50 M to max(\$1100 M)	$\delta = 2.97$ $\rho = 0.146$ $j =$ \$200 M + \$100M to max(\$1600 M)

(conservative to ideal operation) of the total heliostat investment costs is absorbed in the construction of the H_2 production cycle.

With regard to assumed process operation, Scenario 3 uses the cost estimates as shown in Table 2. However, the decrease in Y_3 and the increase in Y_4, results in an increased amount of heat and H_2 required for recovering an increased amount of Mo from its oxide. This together with the decrease in r_{gas} results in an increased amount of gas that has to be processed increasing the number of required NH_3 or H_2 towers respectively. This, altogether, reduces the overall costs per NH_3 tower from 17.6 (Scenario 1) to 16.0 million dollars (Scenario 3) and increases the overall costs per H_2 tower from 81.3 to 92.9 million dollars. Scenario 4 uses the same quantities per tower as that of Scenario 3 with the cost estimates of Scenario 2 resulting in investment costs of 13.4 million dollars per NH_3 tower and 59.4 million dollars per H_2 tower.

3.3. Model evaluation and profitability

The economic feasibility of the plant is determined by its ability to generate a positive net present value (NPV). Given that the only choice variable in the optimization model is NH_3 output, the feasibility analysis presented here is conducted under optimal conditions by multiplying the prevailing price of NH_3 (see 3.1, Fig. 7) by the optimum quantity to get total revenue and adjusting that by operating costs in each period.

The plant is assumed to operate 365 days per annum (in agreement with the annualized solar insulation data employed, see 2.3), running a single labor shift. Assuming an inflation rate of 3%, the cash flows from operations under the four scenarios are estimated. The NPV is then calculated for each scenario using a 10% discount rate. Total operating costs for the year includes labor, service contracts and utilities costs, presented on a per tower basis, as per discussion in Section 3.2. The initial price of the O_2 byproduct is assumed at its current market price of about 21 dollars/t, and allowed to grow naively at the assumed inflation rate of 3% per annum over the simulated 20 year period. Thus, the total plant revenue is enhanced by the revenues emanating from the sale of O_2 in each period. Net revenues are adjusted for corporate taxes to provide the annual cash flow in each period. The economic feasibility based on NPV is presented as:

$$NPV_{lm} = -F_{Z_{lm}} + \sum_{T=1}^{20} \left(\pi_{lmT} (1 + D)^{-T} \right) \tag{7}$$

where D is the discount rate and T is the relevant year.

Fig. 8 displays the NPV and initial plant costs from Scenario 1 or 4 respectively. There exists a pattern of oscillating profitability in both scenarios shown. Scenario 1 shows a negative NPV at the initial output iteration increasing overall as output increases to an NPV of approximately 116.9 million dollars. The 4th iteration's NPV is lower than the 3rd iteration's since, at this point, an increase in output requires an additional H_2 tower and thus allows for only a slight increase in overall output from the 3rd to the 4th iteration with a 116.7 million dollar increase in overall plant costs. This result also appears, albeit at different iterations, for Scenario 4 stemming from the same additional H_2 tower construction requirements. However, Scenario 4 approaches, yet does not reach, a positive NPV within the domain of the model. Since the model is maximizing profit, points at a lower NPV than the previous iteration would not be chosen and output would revert to the previous point. Thus, under the assumptions of Scenario 4 the model suggests the plant does not exist. Fig. 8 shows furthermore the total plant costs vs. output for Scenario 1 or 4 respectively. This illustrates at points where there is excessive unused H_2 output can be increased for a relatively low cost.

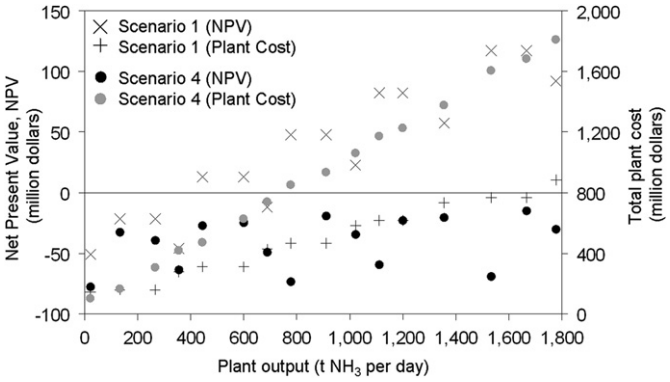

Fig. 8. NPV and total initial plant costs as a function of NH_3 output (for descriptions of scenarios 1 or 4 see 2.3 and 3.2).

Scenario 2 (not shown) yields similar results with Scenario 1, however, the NPV remains at or above 0 within the domain of the model. In contrast, the NPV of Scenario 3 (not shown) is negative at the minimum output simulated and tends further below zero as output increases. This shows the profitability of the plant regardless of the component costs or operational assumptions tends to increase non-linearly in Scenarios 1, 2 and 4.

The high construction cost of the H_2 towers prevents smooth output scaling. It is for this reason that an attempt was made to determine an optimum plant size based upon NPV return per initial capital dollar invested. For this the plant size is limited to model iterations producing approximately 1324 t NH_3 per day (see 2.2) or less using the ratio of NPV over total initial plant costs. This results in an optimum plant size occurring in all four scenarios at the point where H_2 use is maximized or, from constraint 1 in Eq. (6), $X_H - \rho X_N$ is minimized. In Scenario 1 this point is found to yield an NPV return per initial investment dollar of 15.2%. In Scenario 4 the optimum configuration yields a return of −2.1%. Any deviation from this point within the upper and lower boundaries of the model will reduce the NPV to the initial capital ratio. These results are summarized for all four scenarios in Table 6.

Table 6
To outline the optimum plant size: Overall summary of tower quantity, NH_3 output, build costs, net present value (NPV), and the NPV to investment ratio at the scenario-specific configuration optimum (M marks million).

Category	Scenario			
	1	2	3	4
Number of NH_3 towers	19	19	44	44
Number of H_2 towers	5	5	6	6
Output (t NH_3/d)	902.2	902.2	911.2	911.2
Total plant cost (M dollars)	769.9	558.3	1138.6	932.9
NPV (M dollars)	116.9	337.1	−346.6	−19.2
NPV to initial capital ratio (%)	15.2	60.4	−30.1	−2.1

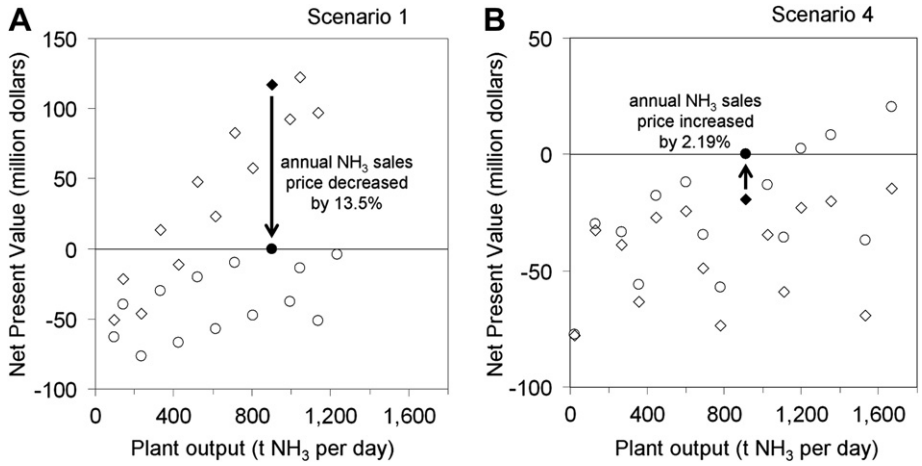

Fig. 9. Sensitivity of (A) Scenario 1 or (B) Scenario 4 to variations in the NH_3 sales price Monte Carlo-simulated over a 20 year plant lifespan (diamonds mark simulations with baseline-NH_3 sales prices, see 3.1 and 3.2, circles mark simulations with in- or decreased NH_3 sales prices, as indicated, to break even at "optimum plant size" shown with filled symbols, see 3.4).

The implications of an optimum plant size as well as the oscillating profit function are potential barriers to entry and deterrents in plant scale changes. The lowest initial required capital to reach an optimum plant size occurs in Scenario 1 at an initial cost of 769.9 million dollars and an output of 902.2 t NH_3 per day. Given this large initial capital requirement for efficient operation operating under the competitive market assumption will in fact generate a fairly large barrier to entry into the market. The oscillation of the profit function implies that careful consideration must be taken before increasing the NH_3 capacity of any plant operating at optimum or at least at a relative maximum in the profit function. Increasing the NH_3 output from either of these points by a fraction will most likely increase the per unit production costs and may even reduce overall profits.

3.4. Sensitivity to the NH_3 sales price

The sensitivity of the presented model to major operational and economic variables is demonstrated analyzing Scenario 1 to 4 (compare Section 2.3 and 3.2) in Section 3.3. To assess the effect of the NH_3 sales price a sensitivity analysis was conducted determining the required NH_3 price to yield an NPV of 0 for all four scenarios within the domain of the model (Fig. 9).

At an optimum output of 902.2 t NH_3 per day, a zero NPV is achieved in Scenario 1 or 2 by decreasing the Monte Carlo simulated 20 year prices (Fig. 7) by 13.5% or 38.8% respectively (Fig. 9A). That is, the possibility of yielding a negative NPV with a fall in the NH_3 sales price is much greater in Scenario 1 than in Scenario 2. On the other hand, at an optimum output of 911.2 t NH_3 per day, Scenario 3 or 4 would require NH_3 sales prices increased by 39.5% in Scenario 3 or 2.19% in Scenario 4 respectively (Fig. 9B). This indicates that in Scenario 4 slight variations in NH_3 prices will result in economic feasibility of the proposed concept. Given in particular the high cost assumptions for acquiring heliostats, Scenario 3 requires a relatively large increase in NH_3 price to "break even".

4. Conclusions and outlook

The solar thermochemical synthesis of ammonia using a molybdenum-based reactant was presented and analyzed from a technical and an economic perspective. Major conclusions are:

- It appears technically feasible to form NH_3 with a reaction cycle conducted at near 0.1 MPa and at $\leq$1500 K and without natural gas or solid reducing agents. This may allow synthesis of artificial nitrogen fertilizer without sophisticated machinery and less depended on the volatility of the natural gas price. As outlined for the U.S., geographical regions with high annual insolation and a relative close supply of coastal or fresh water appear suited for this technology.
- Maximum energy efficiencies of converting solar radiation to the lower heating value of NH_3 were estimated (23–30%) between the efficiency of the industrial NH_3 synthesis employing coal (about 11%) or natural gas (up to 66%). As an aside, this approaches the DOE performance target for solar thermochemical H_2 (i.e., 30% by 2017 or $>$ 35% by 2020 respectively) [33] and includes convenient storage of H_2 in form of NH_3. In the future, research addressing yield and kinetics of the NH_3 formation via materials design [21], heat integration [48], and solar-to-hydrogen technology [33] will be critical for approaching efficiencies realized with the Haber–Bosch process.
- Indirect fossil CO_2 emissions (from coal-derived grid-electricity) are in the range of 4–50% of the CO_2 emitted by the current industrial NH_3 synthesis employing a coal or natural gas feedstock. Yet, no special monetary benefits for technologies utilizing renewable resources via regulations for example for CO_2 emissions are regarded in the analysis presented.
- The cost of heliostats is a major factor determining the economic feasibility of the proposed technology. About 74–86% of the heliostat capital investment is absorbed for H_2 production. Thus, low-cost heliostats (i.e., 90 dollars/m^2) or reduced H_2 reactor costs ($<$16 million dollars, as estimated here), or replacing H_2 with another gaseous reducing agent, may result in a positive NPV (Scenario 4) or augment the return of investment (Scenario 1 or 2 at $>$ 450 t NH_3 per day).
- The sales price increase of NH_3 required for Scenario 4 to break even (2.19%) is below the standard deviation of the Monte Carlo price simulation (5.19%) indicating that an only slightly increased NH_3 market price will further the development of the proposed technology. The present simulation suggests economic feasibility even under conservative assumptions at 534 $\pm$ 28 dollars per ton NH_3. If natural gas prices rise break even will be possible at production levels below 900 t NH_3 per day.
- Production at small scale (144–178 t NH_3 per day when employing only a single H_2 tower) would reduce initial capital requirements (e.g., 770 million dollars at 902 t NH_3 per day,

Scenario 1) and facilitate market entry. Fertilizer production in regions with relatively undeveloped infrastructure, e.g., in developing countries with significant population growth might then be conceivable.

Acknowledgments

This material is based upon work supported by National Science Foundation Grant # 0903701: “Integrating the Socioeconomic, Technical, and Agricultural Aspects of Renewable and Sustainable Biorefining Program, awarded to Kansas State University.” Funding by the Center for Sustainable Energy, Kansas State University is kindly acknowledged.

References

[1] Smil V. Nitrogen and food production: proteins for human diets. Ambio 2002; 31(2):126–31.
[2] Kramer DA. Nitrogen (fixed) - ammonia. US Geological Survey; 2003. Mineral Commodity Summaries pp. 118–119.
[3] Parman BJ, Amanor-Boadu V, Pfromm PH, Michalsky R. Third generation biofuels and the food v. fuel debate: a systems perspective. The International Journal of Environmental, Cultural, Economic and Social Sustainability 2011;2: 287–300.
[4] http://www.ers.usda.gov/Data/FertilizerUse/ [retrieved March 2011].
[5] Gálvez ME, Halmann M, Steinfeld A. Ammonia production via a two-step Al_2O_3/AlN thermochemical cycle. 1. thermodynamic, environmental, and economic analyses. Industrial & Engineering Chemistry Research 2007;46(7): 2042–6.
[6] Thomas G, Parks G. Potential roles of ammonia in a hydrogen economy, a study of issues related to the use ammonia for on-board vehicular hydrogen storage. US Department of Energy, http://www.hydrogen.energy.gov/pdfs/nh3_paper.pdf; 2006 [retrieved December 2011].
[7] Penner SS. Steps toward the hydrogen economy. Energy 2006;31(1):33–43.
[8] Lipman T, Shah N. Ammonia as an alternative energy storage medium for hydrogen fuel cells: scientific and technical review for near-term stationary power demonstration projects (Final research report, UCB-ITS-TSRC-RR-2007-5). Institute of Transportation Studies UC Berkeley Transportation Sustainability Research Center (University of California, Berkeley); 2007.
[9] Christensen CH, Johannessen T, Sørensen RZ, Nørskov JK. Towards an ammonia-mediated hydrogen economy? Catalysis Today 2006;111(1–2): 140–4.
[10] Wang P, Kang XD. Hydrogen-rich boron-containing materials for hydrogen storage. Dalton Transactions 2008;40:5400–13.
[11] Reiter AJ, Kong SC. Combustion and emissions characteristics of compression-ignition engine using dual ammonia-diesel fuel. Fuel 2011;90(1):87–97.
[12] Kirova-Yordanova Z. Exergy analysis of industrial ammonia synthesis. Energy 2004;29(12–15):2373–84.
[13] Panjeshahi MH, Langeroudi EG, Tahouni N. Retrofit of ammonia plant for improving energy efficiency. Energy 2008;33(1):46–64.
[14] Rafiqul I, Weber C, Lehmann B, Voss A. Energy efficiency improvements in ammonia production - perspectives and uncertainties. Energy 2005;30(13): 2487–504.
[15] Ritter SK. The Haber–Bosch reaction: an early chemical impact on sustainability. Chemical & Engineering News 2008;86(33):53.
[16] Yandulov DV, Schrock RR. Catalytic reduction of dinitrogen to ammonia at a single molybdenum center. Science 2003;301(5629):76–8.
[17] Lerch M, Janek J, Becker KD, Berendts S, Boysen H, Bredow T, et al. Oxide nitrides: from oxides to solids with mobile nitrogen ions. Progress in Solid State Chemistry 2009;37(2–3):81–131.
[18] Gálvez ME, Hischier I, Frei A, Steinfeld A. Ammonia production via a two-step Al_2O_3/AlN thermochemical cycle. 3. influence of the carbon reducing agent and cyclability. Industrial & Engineering Chemistry Research 2008;47(7): 2231–7.
[19] Gálvez ME, Frei A, Halmann M, Steinfeld A. Ammonia production via a two-step Al_2O_3/AlN thermochemical cycle. 2. kinetic analysis. Industrial & Engineering Chemistry Research 2007;46(7):2047–53.
[20] Michalsky R, Pfromm PH. Chromium as reactant for solar thermochemical synthesis of ammonia from steam, nitrogen, and biomass at atmospheric pressure. Solar Energy 2011;85(11):2642–54.
[21] Michalsky R, Pfromm PH. Thermodynamics of metal reactants for ammonia synthesis from steam, nitrogen and biomass at atmospheric pressure. (in press, AIChE Journal), http://onlinelibrary.wiley.com/doi/10.1002/aic.13717/pdf.
[22] Auner N, Holl S. Silicon as energy carrier - facts and perspectives. Energy 2006;31(10–11):1395–402.
[23] Steinfeld A, Larson C, Palumbo R, Foley M. Thermodynamic analysis of the co-production of zinc and synthesis gas using solar process heat. Energy 1996; 21(3):205–22.
[24] Steinfeld A, Weimer AW. Thermochemical production of fuels with concentrated solar energy. Optics Express 2010;18(9):A100–11.
[25] Murray JP, Fletcher EA. Reaction of steam with cellulose in a fluidized-bed using concentrated sunlight. Energy 1994;19(10):1083–98.
[26] Lédé J. Reaction temperature of solid particles undergoing an endothermal volatilization - application to the fast pyrolysis of biomass. Biomass & Bioenergy 1994;7(1–6):49–60.
[27] Barin I, Knacke O. Thermochemical properties of inorganic substances. Berlin Heidelberg New York: Springer–Verlag; 1973.
[28] Wise RS, Markel EJ. Synthesis of high-surface-area molybdenum nitride in mixtures of nitrogen and hydrogen. Journal of Catalysis 1994;145(2):344–55.
[29] Cairns AG, Gallagher JG, Hargreaves JSJ, McKay D, Morrison E, Rico JL, et al. The influence of precursor source and thermal parameters upon the formation of beta-phase molybdenum nitride. Journal of Alloys and Compounds 2009; 479(1–2):851–4.
[30] Chen H, Lei XL, Liu LR, Liu ZF, Zhu HJ. Structures and electronic properties of $Mo_{2n}N_n$ ($n = 1–5$): a density functional study. Chinese Physics B 2010;19(12).
[31] Qi J, Jiang LH, Jiang QA, Wang SL, Sun GQ. Theoretical and experimental studies on the relationship between the structures of molybdenum nitrides and their catalytic activities toward the oxygen reduction reaction. Journal of Physical Chemistry C 2010;114(42):18159–66.
[32] Palumbo R, Lédé J, Boutin O, Ricart EE, Steinfeld A, Möller S, et al. The production of Zn from ZnO in a high-temperature solar decomposition quench process - I. the scientific framework for the process. Chemical Engineering Science 1998;53(14):2503–17.
[33] Perret R. Solar thermochemical hydrogen production research (STCH), thermochemical cycle selection and investment priority. Sandia report SAND2011–AND3622. Sandia National Laboratories; 2011.
[34] Lundberg M. Model-calculations on some feasible 2-step water splitting processes. International Journal of Hydrogen Energy 1993;18(5):369–76.
[35] Scott Fogler H. Elements of chemical reaction engineering. Upper Saddle River, NJ: Prentice Hall PTR; 2006.
[36] Balta MT, Dincer I, Hepbasli A. Energy and exergy analyses of a new four-step copper-chlorine cycle for geothermal-based hydrogen production. Energy 2010;35(8):3263–72.
[37] Aspen Plus Ammonia model. Aspen Technology, Inc.; 2008. Version Number V7.0.
[38] http://www.eia.doe.gov/cneaf/electricity/forms/eia920.doc [retrieved 28.01.12].
[39] Sturzenegger M, Nüesch P. Efficiency analysis for a manganese-oxide-based thermochemical cycle. Energy 1999;24(11):959–70.
[40] National Solar Radiation Database, 1991–2005 Update: Typical meteorological year 3, http://rredc.nrel.gov/solar/old_data/nsrdb/1991-2005/tmy3/by_state_and_city.html#C [retrieved 6.01.12].
[41] National Solar Radiation Database 1991 + 2005 Update. User’s manual. technical report NREL/TP-581-41364. online available at:. National Renewable Energy Laboratory http://www.nrel.gov/docs/fy07osti/41364.pdf; 2007 [retrieved 6.01.12].
[42] Perry RH, Green DW, Maloney JO. Perry’s chemical engineers’ handbook. New York: McGraw-Hill; 1984.
[43] Logan JE, Ramendra R. Handbook of turbomachinery. New York: Marcel Dekker, Inc.; 2003.
[44] Maulbetsch JS. Comparison of alternate cooling technologies for California power plants. online available at. California energy Commission and Electrical Power Research Institute (EPRI), Final Report, http://wwwenergycagov/reports/2002-07-09_500-02-079FPDF; February 2002 [retrieved 15.10.07].
[45] Ernst S. Advances in nanoporous materials. Amsterdam: Elsevier; 2009.
[46] http://www.sorbentsystems.com/about.html [retrieved 21.07.11].
[47] Ramezan M, Skone TJ, Nsakala N, Liljedahl GN. Carbon dioxide capture from existing coal-fired power plants. Final report (Original Issue Date, December 2006). National Energy Technology Laboratory; 2007. DOE/NETL-401/110907.
[48] Lapp J, Davidson JH, Lipiński W. Efficiency of two-step solar thermochemical non-stoichiometric redox cycles with heat recovery. Energy 2012;37: 591–600.
[49] Hacker V, Kordesch K. Ammonia crackers. In: Vielstich W, Lamm A, Gasteiger HA, editors. Handbook of fuel cells - fundamentals, technology and applications. Chichester: John Wiley & Sons, Ltd; 2003. p. 121–7.
[50] http://www.lenntech.com/specific-questions-water-quantities.htm [retrieved April, 2011].
[51] http://www.eia.doe.gov/cneaf/electricity/wholesale-/wholesale.html [retrieved April, 2011].